The baculovirus/insect cell system as an alternative to Xenopus oocytes. First characterization of the AKT1 K+ channel from Arabidopsis thaliana

Frédéric Gaymard, Martine Cerutti, Christèle Horeau, Guy Lemaillet, Serge Urbach, Marc Ravallec, Gerard Devauchelle, Herve Sentenac, Jean-Baptiste Thibaud

THE JOURNAL OF BIOLOGICAL CHEMISTRY
Vol. 271, No. 37, Issue of September 13, pp. 22863–22870, 1996

Printed in U.S.A.

The Baculovirus/Insect Cell System as an Alternative to *Xenopus* Oocytes

FIRST CHARACTERIZATION OF THE AKT1 K^+ CHANNEL FROM *ARABIDOPSIS THALIANA**

(Received for publication, February 13, 1996, and in revised form, May 31, 1996)

Frédéric Gaymard‡§, Martine Cerutti¶, Christèle Horeau‡, Guy Lemaillet‡, Serge Urbach‡, Marc Ravallec¶, Gérard Devauchelle¶, Hervé Sentenac‡, and Jean-Baptiste Thibaud‡

From the ‡Laboratoire de Biochimie et Physiologie Moléculaire des Plantes, Ecole Nationale Supérieure Agronomique de Montpellier, Institut National de la Recherche Agronomique, CNRS URA 2133, 34060 Montpellier Cedex 1 and the ¶Laboratoire de Pathologie Comparée, Institut National de la Recherche Agronomique, CNRS URA 1184, 30380 Saint-Christol-les-Alès, France

Two plant (*Arabidopsis thaliana*) K^+ transport systems, KAT1 and AKT1, have been expressed in insect cells (Sf9 cell line) using recombinant baculoviruses. Microscopic observation after immunogold staining revealed that the expressed AKT1 and KAT1 polypeptides were mainly associated with internal membranes, but that a minute fraction was targeted to the cell membrane. KAT1 was known, from earlier electrophysiological characterization in *Xenopus* oocytes, to be an inwardly rectifying voltage-gated channel highly selective for K^+, while similar experiments had failed to characterize AKT1. Insect cells expressing KAT1 displayed an exogenous inwardly rectifying K^+ conductance reminiscent of that described previously in *Xenopus* oocytes expressing KAT1. Under similar conditions, cells expressing AKT1 showed a disturbed cell membrane electrical stability that precluded electrophysiological analysis. Use of a baculovirus transfer vector designed so as to decrease the expression level allowed the first electrophysiological characterization of AKT1. The baculovirus system can thus be used as an alternative method when expression in *Xenopus* oocytes is unsuccessful for electrophysiological characterization of the ion channel of interest. The plant AKT1 protein has been shown in this way to be an inwardly rectifying voltage-gated channel highly selective for K^+ ions and sensitive to cGMP.

In plants, inwardly rectifying potassium channel activity is involved in long-term K^+ uptake and in related functions at the cell or whole plant level, *e.g.* turgor regulation, stomatal guard cell movements, or cell expansion and plant growth (1–3). The first plant K^+ channels characterized at the molecular level, AKT1 (4) and KAT1 (5) from *Arabidopsis thaliana*, were cloned by functional complementation of yeast strains defective in K^+ transport. Several K^+ channels have since been identified using probes from *AKT1* or *KAT1* cDNAs (Refs. 6–8 and sequences found in the EMBL Data Bank). These channels share strong homologies (~60% identity) and show structural and sequence homologies with K^+ channels of the Shaker family found in insects and mammals (4, 5, 9). They display the characteristic hydrophobic domain consisting of six transmembrane segments, named S1 to S6, with a pore-forming region located between S5 and S6. A putative cyclic nucleotide-binding domain is present downstream of S6, as found in cyclic nucleotide-gated channels of the Shaker superfamily (4–8). Two subfamilies can be defined according to the presence or absence (channels of the AKT1 or KAT1 type, respectively) of an ankyrin domain in the polypeptidic chain downstream of the putative cyclic nucleotide-binding domain (3, 4).

Electrophysiological characterization by heterologous expression in *Xenopus laevis* oocytes or yeast indicated that KAT1 is an inwardly rectifying voltage-gated K^+ channel highly selective for K^+ (10–15). It is expressed in guard cells and thought to mediate long-term K^+ influx leading to stomatal opening (16). Northern blot analysis indicated that *AKT1* is expressed mainly in roots (17). Studies of its tissue-specific expression using the *GUS* reporter gene revealed that its promoter directs preferential expression in the peripheral cell layers of the mature region of roots (18), suggesting a role in K^+ uptake from the soil solution. Injection of *AKT1* cRNA in *Xenopus* oocytes did not, however, affect the membrane conductance.[1] The K^+ channel activity of the encoded polypeptide thus awaited characterization.

The insect cell line Sf9 can express high levels of foreign proteins when infected by a recombinant baculovirus. This expression system has been shown to be capable of performing most eukaryotic post-translational modifications (19, 20). It has been used, in particular, for expressing the *Drosophila* Shaker K^+ channel in a functional form (21–23). In this study, functional expression of AKT1 and KAT1 polypeptides has been achieved using the baculovirus/Sf9 system.

EXPERIMENTAL PROCEDURES

Antibodies—Polyclonal antibodies were raised against the ankyrin domain of AKT1 and the C-terminal region of KAT1 (see Fig. 1A). Nucleotide sequences coding for these domains were cloned into the pET-3c vector designed for expression in *Escherichia coli* (24). The required restriction sites (*Nde*I and *Bam*HI) were introduced in *AKT1* and *KAT1* cDNAs as described below.

The ankyrin domain of AKT1 was amplified by polymerase chain reaction using a 5′-primer (5′-TTTCATATGGATCTTCCTCTC) introducing a *Nde*I site at position 1600 of *AKT1* cDNA and a 3′-primer (5′-GGAACCGGATCCCGGTTTAGAGTATAGG) introducing a TAA stop codon at position 2218, just before the unique *Bam*HI site present in *AKT1*. The *Nde*I-*Bam*HI fragment was sequenced on both strands. *KAT1* cDNA was introduced into pBluescript® so that the *Bam*HI polylinker site was present downstream of the *KAT1* stop codon. The

* This work was supported in part by the Bio Avenir Programme funded by Rhône-Poulenc and the Ministry in Charge of Research and Industry and by the European Community BIOTECH Program as part of the Project of Technological Priority 1993–1996. The costs of publication of this article were defrayed in part by the payment of page charges. This article must therefore be hereby marked "*advertisement*" in accordance with 18 U.S.C. Section 1734 solely to indicate this fact.

§ To whom correspondence should be addressed. Tel.: 33-67612518; Fax: 33-67525737; E-mail: gaymard@ensam.inra.fr.

[1] C. Bosseux, J.-B. Thibaud, and A.-A. Véry, unpublished data.

*Nsi*I-*Bam*HI fragment encoding the C-terminal part of KAT1 was cloned into the pJRD184 vector (25), introducing a *Nde*I site just upstream of the *Nsi*I site. The *Nde*I-*Bam*HI fragment was thereafter introduced into the pET-3c vector.

The recombinant pET-3c vectors were introduced in *E. coli* strain BL21(DE3) (24). Protein expression was induced by adding isopropyl-1-thio-β-D-galactopyranoside (final concentration of 0.4 mM) and lasted 3 h at 37 °C. Both expressed polypeptides formed inclusion bodies (26). They were purified by washing the inclusion bodies several times with a medium containing 50 mM Tris-HCl (pH 8), 2 mM EDTA, 1 M NaCl, and 5% Triton X-100. The final pellet was suspended in 50 mM Tris-HCl (pH 8), 2 mM EDTA, 0.5 mM dithiothreitol, and 7 M urea. Approximately 40 μg of proteins were subjected to SDS-PAGE.[2] Acrylamide bands containing overexpressed polypeptides were crushed in 2 ml of PBS, and the resulting mixtures were used to immunize rabbits intradermally. Booster injections were given 2 months later.

Insect Cell Culture—The Sf9 cell line was maintained in monolayer culture at 28 °C in TC-100 medium (Life Technologies, Inc.) supplemented with 0.37 g/liter α-ketoglutaric acid, 0.4 g/liter β-D-fructose, 0.055 g/liter fumaric acid, 0.67 g/liter malic acid, 0.06 g/liter succinic acid, 2.7 g/liter sucrose, 0.2 g/liter choline chloride, 0.2 g/liter β-alanine, 0.35 g/liter $NaHCO_3$, 3.33 g/liter lactalbumin (Difco), 0.05 g/liter streptomycin sulfate, 0.125 g/liter penicillin, and 10% fetal calf serum. Cells were split every 4 days to maintain a density ranging from $\sim 4 \times 10^4$ to 7×10^5 cells/ml.

Recombinant Baculoviruses—Two baculovirus transfer vectors (see Fig. 1*B*) were used, pGmAc34T (27) and pGmAc217. In the pGmAc34T vector, the initiator ATG codon of polyhedrin was removed by changing G to T, a *Not*I cloning site was introduced at position +45 (position +1 is the first nucleotide of the polyhedrin initiator ATG codon), and residues +45 to +462 were deleted. In the pGmAc217 vector, residues −8 to +502 were deleted, and a *Bgl*II site was introduced just downstream to position −8. Such a deletion in the promoter region has been shown to result in a decreased expression level (28).

Recombinant transfer vectors, named p34T-AKT1, p34T-KAT1, and p217Δ-AKT1, were obtained as described in the legend to Fig. 1*B* by cloning *AKT1* and *KAT1* cDNAs into pGmAc34T and *AKT1* cDNA into pGmAc217, respectively. Sf9 cells were transfected with wild-type viral DNA and the recombinant transfer vector p34T-AKT1, p34T-KAT1, or p217Δ-AKT1 using *N*-[1-(2,3-dioleoyloxy)propyl]-*N*,*N*,*N*-trimethylammonium methylsulfate (Boehringer Mannheim) as fusion agent according to Davrinche *et al.* (27). Recombinant baculoviruses were purified and named RB34T-AKT1, RB34T-KAT1, and RB217Δ-AKT1, respectively. They were amplified to 10^8 plaque-forming units/ml and used for protein expression.

Membrane Purification—Sf9 cells in exponential phase were layered at a density of 5×10^5 cells/ml and infected with recombinant baculoviruses at a multiplicity of infection of 10. After 2 days of incubation at 28 °C, cells were harvested and centrifuged at 500 × *g* for 5 min. The pellet was washed with ice-cold PBS. The cells were centrifuged for 5 min at 500 × *g* and resuspended at $\sim 10^7$ cells/ml in a grinding medium containing 10 mM Tris-HCl (pH 7.5), 1 mM EDTA, 250 mM NaCl, 10% glycerol, 1 mM dithiothreitol, 2 mM phenylmethylsulfonyl fluoride, 2 μg/ml aprotinin, 1 μg/ml leupeptin, 1 μg/ml pepstatin, and 1 μg/ml antipain. The suspension was frozen in liquid nitrogen, quickly thawed at room temperature, and sonicated three times for 10 s with a probe sonicator. The homogenate (referred to as total extract) was centrifuged twice at 13,000 × *g* for 20 min. The supernatant was collected and centrifuged at 100,000 × *g* for 1 h. The crude membrane pellet was suspended in 2 mM Tris-HCl (pH 7.5), 1 mM dithiothreitol, 2 mM phenylmethylsulfonyl fluoride, and 10% glycerol and stored in liquid nitrogen. Proteins were assayed according to Schaffner and Weissman (29) using bovine serum albumin as a standard.

Immunoblots—Proteins were separated by SDS-PAGE according to Laemmli (30) and electroblotted onto a nitrocellulose membrane (Sartorius Corp.) at 100 V for 1 h in a medium containing 25 mM Tris, 192 mM glycine, 0.1% SDS, and 20% methanol. Blots were blocked in PBS containing 5% low fat milk for 3 h at room temperature. Primary antibody diluted in PBS containing 0.1% Tween 20 (PBS-T) was bound overnight at room temperature. After three 10-min washes in PBS-T, goat anti-rabbit IgG secondary antibody coupled to peroxidase (Sigma) diluted in PBS-T was added. Blots were incubated for 2 h at room temperature and washed as described above. Peroxidase activity was detected using a 0.5 mg/ml 4-chloronaphthol solution prepared in PBS, 20% methanol, and 0.015% H_2O_2.

Immunogold Staining and Microscopy—Sf9 cells were infected with recombinant baculoviruses as described above (see "Membrane Purification") and harvested 2 days later by pelleting at 500 × *g* for 5 min. They were fixed for 1 h in 4% paraformaldehyde in PBS at 4 °C. Following dehydration (increasing ethanol concentration up to 100%), cells were embedded in LR white resin (Taab). Thin sections were made and immunostaining was performed as described (31). Observations were made with a Zeiss (Jena) EM 10C/CR electron microscope.

Patch-clamp Experiments—Sf9 cells were plated in 3-cm diameter cell culture dishes and infected as described above (see "Membrane Purification"). Prior to electrophysiological recordings, culture medium was replaced by a bath solution containing 10 mM KCl (or 100 mM KCl), 4 mM $CaCl_2$, 5 mM $MgCl_2$, 5 mM glucose, 10 mM MES/Tris (pH 6.3), and NaCl (to give an osmolality of 0.28). Standard voltage-clamp protocols (see "Results") allowed macroscopic current recording in the whole cell configuration of patch-clamp (32).

Micropipettes were two-step pulled from soft glass (Modulohm A/S, Herleu, Denmark) and displayed typically a 2-megaohm resistance in bath solution when filled with 60 mM KF, 50 mM KCl, 1 mM $MgCl_2$, 10 mM EGTA, 10 mM MOPS/NaOH (pH 7.2), and NaCl (osmolality set to 0.30). Reference and measuring electrodes were connected to an Axopatch 200 A amplifier that was controlled by pClamp software (Axon Instruments, Inc.). Linear leak current was digitally subtracted from recorded whole cell current. Most capacitive currents could usually be compensated by using built-in features of the amplifier. Residual capacitive currents were recorded and digitally subtracted from whole cell currents using the method described by Zittlau and Walther (33). Digitized data were analyzed using pClamp and Sigmaplot (Jandel Scientific, Erkrath, Germany) software.

RESULTS

Expression of KAT1 and AKT1—Sf9 cells were infected either with wild-type baculovirus or with viruses recombinant for *KAT1* or *AKT1* cDNA: RB34T-KAT1, RB34T-AKT1, and RB217Δ-AKT1 (see "Experimental Procedures" and Fig. 1). RB217Δ-AKT1 was obtained using a transfer vector designed (deletion in the polyhedrin promoter) (Fig. 1) so as to decrease the level of expression of the foreign sequence.

Infection of Sf9 cells with wild-type baculovirus resulted in the appearance of many extra bands following SDS-PAGE of total cell extract (Fig. 2*A*). The major one, present at 31 kDa, corresponds to the virus polyhedrin gene product. When Sf9 cells were infected with viruses recombinant for *KAT1* or *AKT1* cDNA, the polyhedrin band was no longer present, while an extra major band was clearly visible. The relative molecular mass of this band was close to that expected for the corresponding plant channel: ~70 kDa for KAT1 (predicted molecular mass of 78 kDa) and 95 kDa for AKT1 (predicted molecular mass of 97 kDa) (Fig. 2*A*). Antibodies raised against KAT1 or AKT1 detected a 70-kDa band (Fig. 2*B*, *lane 34T-KAT1*) and a 95-kDa band (*lanes 34T-AKT1* and *217Δ-AKT1*), respectively. This confirmed that both plant channels were expressed in Sf9 cells. The level of expression of AKT1 was lower in RB217Δ-AKT1-infected cells than in RB34T-AKT1-infected cells, as expected from the use of an 8 base pair-deleted polyhedrin promoter (28).

Plant Channel Targeting in Sf9 Cells—In a preliminary biochemical approach, the cellular localization of plant channels expressed in Sf9 cells was investigated by preparing soluble and membrane protein fractions and analyzing their polypeptide composition by SDS-PAGE. Polypeptide bands of the size expected for AKT1 and KAT1 were detected in the membrane protein fraction (Fig. 3). Western blotting performed with the corresponding antisera failed to detect the channels in the soluble protein fraction (Fig. 3*B*).

The cellular distribution of AKT1 in Sf9 cells was further investigated by immunogold staining. Infection with *AKT1* and *KAT1* recombinant viruses dramatically increased the amount of intracellular membrane (Fig. 4) when compared with that of

[2] The abbreviations used are: PAGE, polyacrylamide gel electrophoresis; PBS, phosphate-buffered saline; MES, 4-morpholineethanesulfonic acid; MOPS, 4-morpholinepropanesulfonic acid.

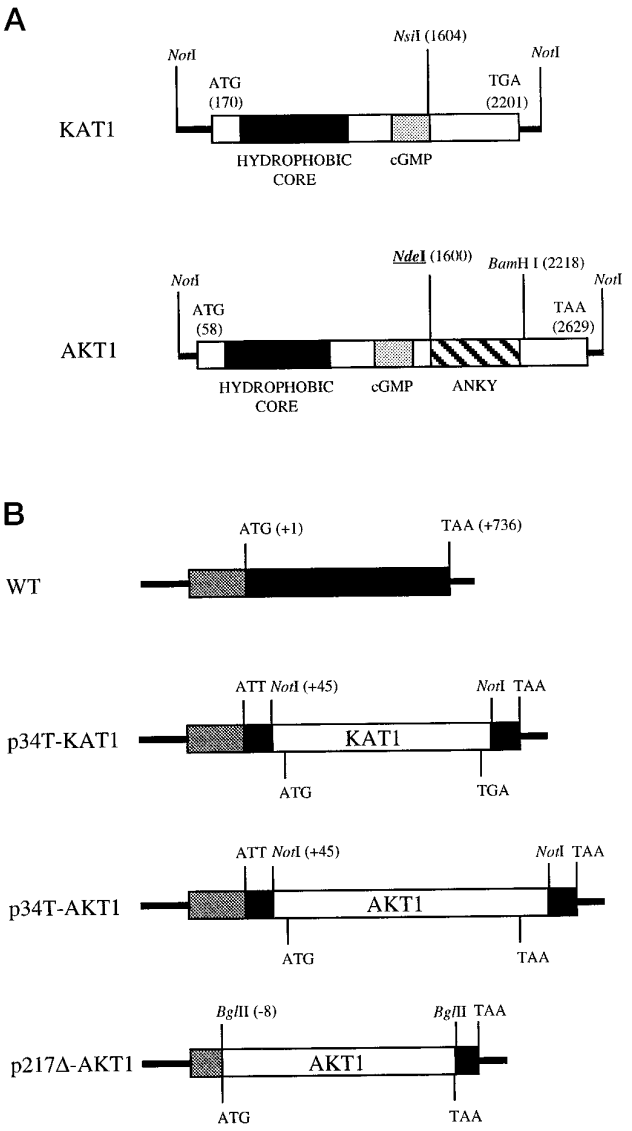

FIG. 1. **Construction of *E. coli* expression vectors and of baculovirus transfer vectors.** *A*, *KAT1* and *AKT1* cDNAs (EMBL Data Bank accession numbers X93022 and X62907) flanked by *Not*I sites, obtained by *Not*I digestion of clones isolated from the yeast expression *A. thaliana* cDNA library (41). *Black box*, cDNA domain encoding the channel hydrophobic core including the six membrane-spanning segments; *gray box*, cGMP-binding domain; *striped box*, ankyrin (*ANKY*) domain of AKT1 (for sequence analysis, see Refs. 4 and 9). The C-terminal region of KAT1 and the ankyrin domain of AKT1 were expressed in *E. coli* using the pET-3c vector, the coding sequences being introduced between the *Nde*I and *Bam*HI cloning sites (see "Experimental Procedures"). The positions of the *KAT1* and *AKT1* initiator ATG and stop codons and those of the restriction sites used for this work are indicated. The C-terminal region of KAT1 expressed in *E. coli* begins at the *Nsi*I site present at position 1604 and ends with the stop codon of the protein. To produce the ankyrin domain of AKT1, an *Nde*I site (*underlined*) and a stop codon just upstream of the *Bam*HI site were introduced by polymerase chain reaction. *B*, diagrammatic representation of the transfer vectors used to obtain recombinant baculoviruses. *KAT1* and *AKT1* cDNAs were cloned downstream of the promoter of the baculovirus polyhedrin gene. Numbering is given using position +1 for the first nucleotide of the polyhedrin initiator ATG codon. *WT*, wild-type baculovirus polyhedrin gene region. *Gray* and *black boxes*, the promoter and open reading frame, respectively, of the polyhedrin gene. p34T-KAT1 and p34T-AKT1 are transfer vectors obtained by cloning *KAT1* and *AKT1* cDNAs into pGmAc34T, respectively. p217Δ-AKT1 was obtained by cloning *AKT1* cDNA into pGmAc217. *Bgl*II sites were introduced upstream of the initiator codon and downstream of the stop codon of AKT1 by polymerase chain reaction.

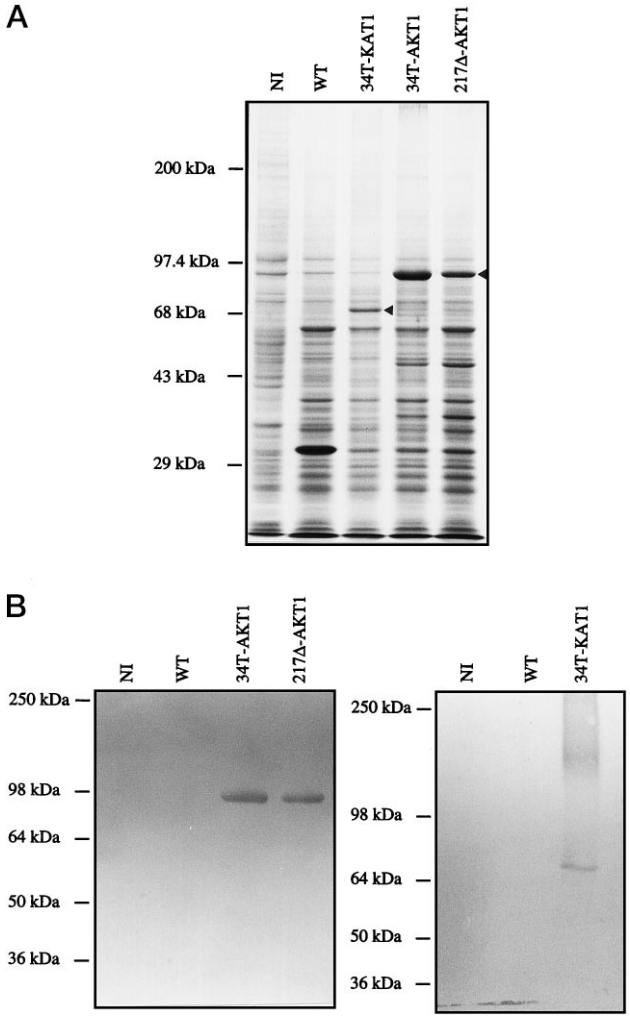

FIG. 2. **Expression of KAT1 and AKT1 in Sf9 cells.** *Lanes NI* and *WT*, total extract from uninfected cells and wild-type baculovirus-infected cells, respectively; *lanes 34T-KAT1*, *34T-AKT1*, and *217Δ-AKT1*, total extract from cells infected with RB34T-KAT1, RB34T-AKT1, and RB217Δ-AKT1, respectively. *A*, Coomassie Blue-stained gel. Extracts (60 μg of protein) were subjected to SDS-PAGE (8–15% polyacrylamide gel). The positions of AKT1 and KAT1 are indicated by arrowheads. *B*, Western blots. *Lanes NI* and *WT* contained 10 μg of protein. *Lanes 34T-KAT1*, *34T-AKT1*, and *217Δ-AKT1* contained 2 μg of protein. Blots were probed using a serum directed against the ankyrin domain of AKT1 (*left*) or a serum directed against the C-terminal part of KAT1 (*right*) (see Fig. 1).

control cells (uninfected or infected with wild-type virus) (data not shown). Strong staining was observed in both RB34T-AKT1- and RB217Δ-AKT1-infected cells (Fig. 4, *A–D*), in contrast to control cells. Additionally, KAT1-expressing cells (RB34T-KAT1-infected) probed with the serum raised against the AKT1 ankyrin domain (Fig. 4*E*) also showed little staining, equivalent to that observed with the other controls. High magnification micrographs (Fig. 4, *C–D*) indicated that most AKT1 proteins had an intracellular localization in both cells and that only a minute fraction of the expressed polypeptide was targeted to the plasma membrane. The intracellular pool of AKT1 was associated with internal membranes. Counting of gold particles was performed on nine different cells of each type. While internal membrane staining in RB217Δ-AKT1-infected cells was 35% lower than in RB34T-AKT1-infected cells (24 and 37 particles/μm^2, respectively; S.D. $< 20\%$ of mean values), plasma membrane staining was similar in both cell types ($\sim 2.7 \pm 0.8$ particles/μm of plasma membrane) (data not shown).

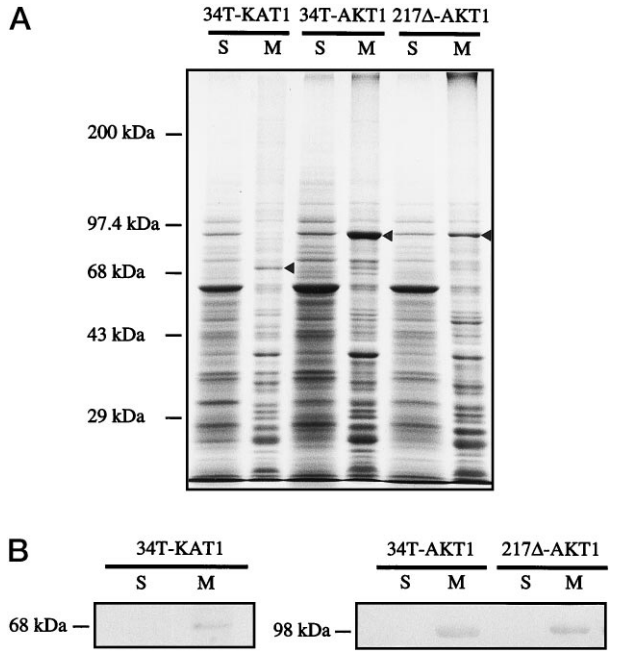

FIG. 3. **Targeting of KAT1 and AKT1 polypeptides to the membrane fraction.** *Lanes 34T-KAT1*, *34T-AKT1*, and *217Δ-AKT1*, cells infected with RB34T-KAT1, RB34T-AKT1, and RB217Δ-AKT1, respectively. Cells were collected at 48 h postinfection and broken by sonication. The homogenate was subjected to centrifugation (2 × 13,000 *g* for 20 min and 100,000 × *g* for 1 h). Soluble (supernatant) (*lanes S*) and microsomal (pellet) (*lanes M*) fractions were collected and loaded on a polyacrylamide gel. *A*, Coomassie Blue-stained gel. Each lane contained 60 μg of protein. *B*, Western blots. Lanes contained either 10 μg of microsomal protein or 30 μg of soluble protein. Blots were probed using a serum directed against the C-terminal part of KAT1 (*left*) or a serum directed against the ankyrin domain of AKT1 (*right*) (see Fig. 1).

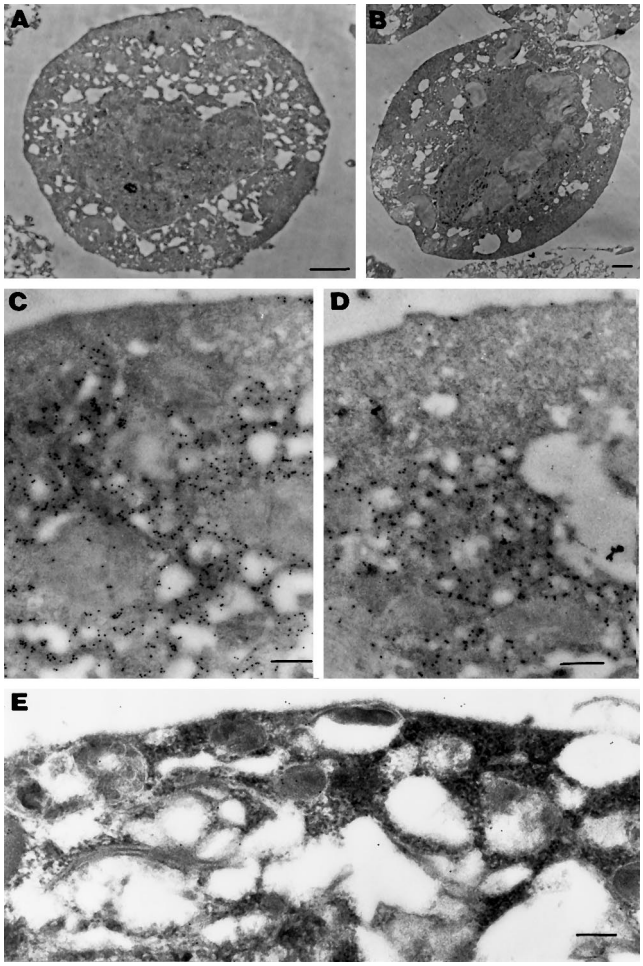

FIG. 4. **AKT1 localization in Sf9 cells.** Cells were harvested, fixed with paraformaldehyde, and embedded in resin. Thin sections were probed with a serum directed against the ankyrin domain of AKT1 and with a gold-conjugated anti-rabbit IgG. *A*, RB34T-AKT1-infected cell (*bar* = 1 μm); *B*, RB217Δ-AKT1-infected cell (*bar* = 1 μm); *C* and *D*, magnification of the cell shown in *A* and *B*, respectively (*bar* = 0.2 μm); *E*, control (cell expressing KAT1 (RB34T-KAT1-infected) probed with the serum directed against AKT1) (*bar* = 0.2 μm).

Electrophysiological Evidence for Functional Channel Expression—From a holding potential of −10 mV, membrane potential was clamped for 800-ms periods to values ranging from 0 to −160 mV. Negligible currents were usually recorded in cells infected with wild-type virus as shown in Fig. 5*A*. In some cell batches, however, randomly activating currents could be recorded at membrane potential values negative to −120 mV (data not shown). Cell batches that exhibited this behavior were discarded.

Slowly activating inward currents could be recorded in cells infected with each of the recombinant viruses (Fig. 5, *B–D*). During double-pulse protocols, the above three cell types displayed tail currents that reversed at potential values close to the equilibrium potential for K^+ ions (data not shown, but see Fig. 6 and Table I regarding RB217Δ-AKT1-infected cells), indicating that the inward currents shown in Fig. 5 were mainly carried by K^+ ions. As current recording was much more reproducible in cells expressing AKT1 from RB217Δ-AKT1 (Fig. 5*D*) than from RB34T-AKT1 (Fig. 5*C*), AKT1 channel activity was further characterized using the former virus.

AKT1 Channel Selectivity—Deactivating currents were recorded during 500-ms pulses, following a 800-ms activating pulse at −150 mV. As the reversal potential of current through AKT1 channels was expected to lie close to the K^+ equilibrium potential, the deactivating pulse potential ranged from −90 to −20 mV when the external solution contained 10 mM K^+ and from −40 mV to +30 mV when it contained 100 mM K^+. Typical results are shown in Fig. 6, and mean values for the reversal potential are given in Table I. The mean reversal potential shifted by 57 mV following a change in the bathing K^+ concentration from 10 to 100 mM (pipette solution contained 110 mM K^+ in both cases).

AKT1 Channel Voltage Gating—Inward currents were recorded during hyperpolarizing pulses in cells bathed first in 10 mM K^+ and thereafter in 100 mM K^+. These currents activated slowly with a multiexponential time course (Fig. 7, *A* and *B*). Steady-state activation was virtually achieved within the 1100-ms hyperpolarizing pulses. Half-activation time was clearly voltage-dependent: 40 ms at −180 mV and 160 ms at −120 mV in the 10 mM K^+ bath (36 and 140 ms, respectively, in 100 mM K^+). Plotting steady-state current *versus* voltage (Fig. 7*C*) revealed a strong inward rectification. Due to the presence of a Shaker S4-like voltage sensor in AKT1 (4), we hypothesized that this rectification was due mainly to a voltage-dependent G/G_{max} ratio and determined whether the steady-state *I/V* curves shown in Fig. 7*C* could be fitted by a simplified voltage-gating model. As described previously for the KAT1 channel (12), the steady-state current was assumed to be predicted by the Goldman equation, multiplied by a voltage-dependent G/G_{max} ratio changing from 0 to 1 upon hyperpolarization. The G/G_{max} voltage dependence was described using a simple two-state Boltzmann equation, assuming it was independent of the K^+ concentration in the bath (10 or 100 mM). The calculated steady-state *I/V* curve was drawn in full line in Fig. 7*C* for each bath condition. The single Boltzmann curve corresponding to both fits is shown in Fig. 7*D*. The half-activa-

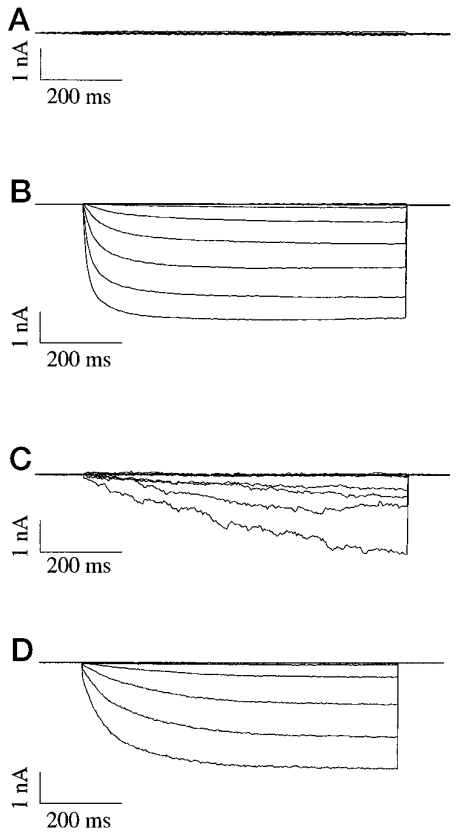

FIG. 5. **Whole cell currents recorded in baculovirus-infected Sf9 cells.** Cells were infected at a multiplicity of infection of 10 with wild-type baculovirus (*A*) or with RB34T-KAT1 (*B*), RB34T-AKT1 (*C*), or RB217Δ-AKT1 (*D*). Currents were recorded 2 days later. The bath contained 100 mM KCl, 4 mM $CaCl_2$, 5 mM $MgCl_2$, 5 mM glucose, 10 mM MES/Tris (pH 6.3), and NaCl (amount required for an osmolality of 0.28). The pipette solution contained 60 mM KF, 50 mM KCl, 1 mM $MgCl_2$, 10 mM EGTA, 2 mM MgATP, 10 mM MOPS/NaOH (pH 7.2), and NaCl (to give an osmolality of 0.30). From a holding potential of −10 mV, the membrane was clamped at values ranging from 0 to −160 mV, with a step of −20 mV during nine 800-ms-long successive pulses.

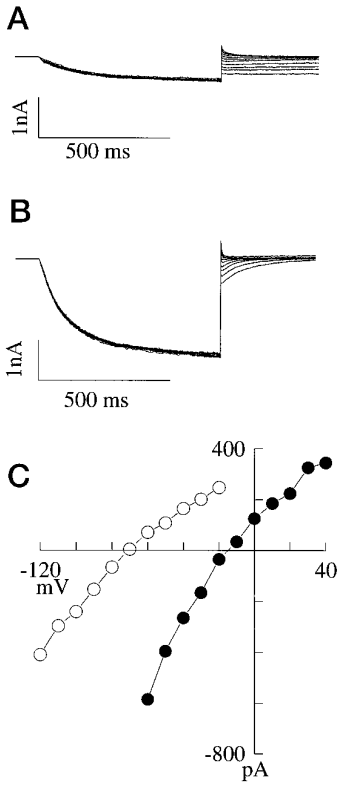

FIG. 6. **Deactivating currents recorded in RB217Δ-AKT1-infected Sf9 cells and instantaneous current/voltage curve.** The bath solution contained either 10 mM KCl (*A*) or 100 mM KCl (*B*). *A* and *B*, currents recorded during double-pulse protocols. Holding potential was 0 mV. The activating pulse at −150 mV lasted 800 ms. Tail currents were recorded in the −20 to −120 mV range in 10 mM K^+ bath solution (*A*) and in the 40 to −60 mV range (10-mV step) in 100 mM K^+ bath solution (*B*). Leak and capacitive currents were mathematically subtracted after recording. *C*, instantaneous deactivating current plotted against voltage applied during the second pulse of the voltage-clamp protocol. The data are from *A* (○) and *B* (●).

tion potential is −123 mV, and the equivalent gating charge is 1.5.

Effect of ATP and cGMP on AKT1 Activation—In most cases, a rapid decrease in AKT1 current was observed when the pipette solution contained no ATP (Fig. 8*A*). This decrease could generally be prevented by including 2 mM ATP in the pipette solution (Fig. 8*B*). The standard pipette solution thus contained 2 mM MgATP. In some cases, this ATP concentration caused an increase in the current recorded at a given potential. This was due to a slight positive shift in the activation potential (Fig. 8*B*). When the clamped cell was perfused with a bath solution supplemented with 0.1 mM 8-bromo-cGMP, the current decreased. This was due to a negative shift in the activation potential, as shown in Fig. 8*C* (example representative of six independent recordings). This shift in AKT1 activation potential was time-dependent; the maximal value was reached within ~15 min and was in the −25 to −40 mV range.

DISCUSSION

Our current knowledge of the structure/function relationship of voltage-gated animal Shaker channels originates mainly from the literature reporting the functional characterization of wild-type and mutant channels expressed in *Xenopus* oocytes. This expression system is popular for electrophysiologists as it is readily amenable to current recordings. However, in some unpublished experiments aimed at characterizing new putative animal channels, no functional expression has been obtained from cRNA injection in oocytes.[3] Similarly, although the KAT1 channel was expressed and characterized in *Xenopus* oocytes (10–14), similar attempts for AKT1 have failed up until now.

TABLE I
Reversal potential of AKT1 current compared with theoretical K^+ equilibrium potential

Data for the reversal potential of the AKT1 current were obtained from instantaneous deactivating currents recorded after a 800-ms-long activating prepulse at −150 mV and are given as mean ± S.D. (number of determinations). The theoretical K^+ equilibrium potential was derived from the Nernst equation, assuming that the cell K^+ concentration is that of the pipette solution.

	Bath/pipette K conc	
	10/110 mM	100/110 mM
	mV	
Reversal potential of AKT1 current	−63 ± 9 (10)	−5 ± 4 (7)
Theoretical K^+ equilibrium potential	−62	−2

The baculovirus/insect cell system has often been used to express functional membrane proteins (20). The *Drosophila* Shaker K^+ channel was shown to be expressed in Sf9 cells and targeted to the plasma membrane in a functional state (21). KAT1 and AKT1 are the first ion channels from the plant kingdom to be expressed using this system. Both plant chan-

[3] O. Pongs, personal communication.

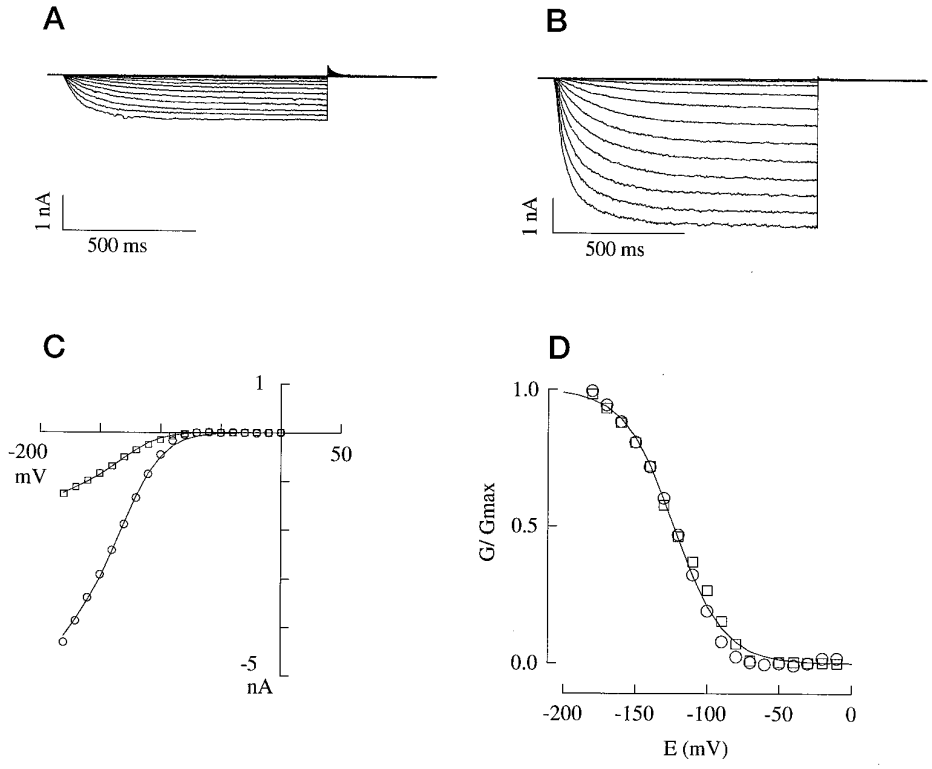

FIG. 7. **Voltage gating is the major mechanism underlying inward rectification of AKT1 channels.** *A* and *B*, whole cell currents recorded in RB217Δ-AKT1-infected Sf9 cells. The bath contained 10 mM KCl (*A*) or 100 mM KCl (*B*). Holding potential was 0 mV. Voltage-clamp episodes lasted 1100 ms, and clamp potential ranged from 0 to −180 mV with a −10-mV step. *C*, steady-state current through AKT1 channels plotted against membrane potential. The steady-state current value was taken at the end of the voltage-clamp episode on current traces shown in *A* (□) and *B* (○). *Full line curves* represent the prediction of the voltage-gated channel theory (see "Results"). *D*, dependence of G/G_{max} on membrane potential. *Squares* and *circles* represent G/G_{max} values calculated from the data shown in *C*. The *full line curve* represents the voltage-dependent variation of G/G_{max} predicted by the Boltzmann law (see "Results").

nels have been expressed in a functional form and partly targeted to the plasma membrane of the cells as revealed by whole cell current recording and immunogold staining (Figs. 4–8). This is the first report showing that the baculovirus expression system can be used in an alternative strategy for characterizing ion channels when attempts using *Xenopus* oocytes have failed. The reason why AKT1 is expressed in a functional state in the former system and not in the latter is still unknown.

The membrane of Sf9 cells was often unable to withstand hyperpolarizations beyond −100 mV. Due to this problem, Sf9 cells do not offer the ideal system for electrophysiological characterization of hyperpolarization-activated channels such as KAT1 and AKT1. Some cell batches, however, were able to withstand membrane potential as negative as −160 mV (Fig. 5*A*) or even −180 mV. It is worth noting that Sf9 cells infected with either RB34T-KAT1 or RB217Δ-AKT1 recombinant baculovirus withstood large hyperpolarizations (see Fig. 6 for RB217Δ-AKT1-infected cells) much more reproducibly than wild-type baculovirus-infected cells or RB34T-AKT1-infected cells.

AKT1 was highly expressed in cells infected with RB34T-AKT1 (Fig. 2); however, these cells showed membrane instability. Breakdowns occurred especially at potentials more negative than −100 to −120 mV, precluding any characterization of AKT1 channel activity using this construct (Fig. 5*C*). As expected, the expression level of AKT1 in cells infected with RB217Δ-AKT1 was lower than in the former cells (Fig. 2). In both types of cells, the plant channel was present in the membrane fraction (Fig. 3), although the amount of AKT1 actually targeted to the plasma membrane was small and roughly the same in both cases (Fig. 4). Most expressed polypeptides remained associated with internal membranes; their functional competence is unknown. A similar phenomenon with the expression of the *Drosophila* Shaker channel in Sf9 cells was hypothesized from the discrepancy between the magnitude of the currents recorded in the infected cells and the intensity of the Shaker polypeptide band on a Coomassie Blue-stained protein gel (21). Similarly, a liver gap junction protein expressed in Sf9 cells has been shown to remain mainly associated with the endoplasmic reticulum, with only a small fraction reaching the cell surface (34). It seems that Sf9 cells are able to synthesize large amounts of membrane proteins, but the protein export machinery is overwhelmed by the high rates of synthesis (35).

By making use of the RB217Δ-AKT1 virus instead of the RB34T-AKT1 virus, it was possible to obtain conditions allowing the functional characterization of AKT1. This work represents the first data on AKT1 channel activity. Our results demonstrated that the reversal potential for AKT1 current remained close to the equilibrium potential for K^+ ions when the external concentration of this ion was changed (Table I), indicating that this current is mainly carried by K^+ ions. This is in agreement with the presence in the putative selectivity filter-forming region of a GYGD motif (4) thought to be a hallmark of highly selective K^+ channels (36).

Like KAT1 current, AKT1 current activated slowly upon hyperpolarization and underwent no inactivation (Fig. 5). Comparison of traces in Fig. 5*D* to those in Fig. 5*B* reveals that AKT1 activation was slower than that of KAT1 and occurred from a more negative threshold potential. It should be noted, however, that KAT1 activation in Sf9 cells was faster (half-activation time of ~15 ms at −140 mV) (Fig. 5*B*) than that observed in *Xenopus* oocytes (half-activation time of ~200 ms at −140 mV) (11). Thus, the kinetic features of KAT1 are dependent on the expression system used. This might be due to

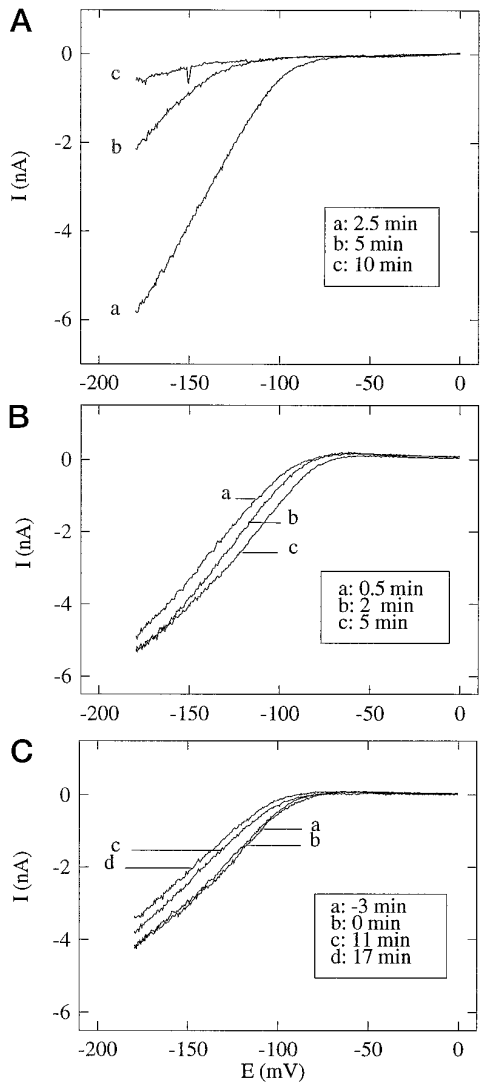

FIG. 8. **AKT1 channel activation is ATP-dependent and cGMP-sensitive.** Voltage ramps (from 0 to −180 mV within 10 s) were applied to the membrane of RB217Δ-AKT1-infected Sf9 cells at time intervals after rupturing the patch. Pseudo steady-state current/voltage curves could be recorded. *A*, the absence of ATP in the pipette solution (same as given in the legend to Fig. 5, but without MgATP) caused a rapid decrease in AKT1 inward current. Zero time was at rupturing the patch. The bath contained 100 mM K^+ (same as for Fig. 7*B*). *B*, a 2 mM MgATP pipette solution prevented the time-dependent decrease in current. Successive *I*/V ramps shifted positively along the voltage axis. Zero time was at rupturing the patch. *C*, the addition of 100 μM 8-bromo-cGMP at zero time (upon recording the *b ramp*, 8 min after rupturing the patch) made the further *I*/V ramps shift negatively along the voltage axis.

differences in expression levels in *Xenopus* oocytes and Sf9 cells since differences in the expression level of KAT1 within the same expression system (*Xenopus* oocytes) have been shown to result in changes in the kinetic features of this channel (11). Similarly, features of the *Drosophila* Shaker K^+ channel have been shown to depend on the expression system used: the activation curves are qualitatively identical in Sf9 cells and *Xenopus* oocytes, but the curve obtained in the former system is shifted ~15 mV to more depolarized potentials (21). Whether these kinds of differences are relevant or not to the regulation and the role of the channel *in situ* in the animal/plant is as yet unknown (11, 37).

As shown in steady-state *I*/V curves (Fig. 7*C*), AKT1 displayed a strong inward rectification. This is likely to originate mainly from some voltage-dependent gating as shown by the Boltzmann fit in Fig. 7*D*. The presence of ATP in the pipette solution was required to obtain routinely a stable AKT1 activation upon repeated hyperpolarizations. AKT1 current decrease in the absence of ATP was variable between cells (in the example of Fig. 8*A*, the decrease was particularly fast). ATP (2 mmol/liter) generally shifted the *I*/V curve positively along the voltage axis (Fig. 8*B*). A shift of this curve in the opposite direction was elicited by bathing the cell with 100 μM 8-bromo-cGMP solution (Fig. 8*C*). All but one of these observations are reminiscent of those recently reported regarding KAT1 expressed in oocytes: while the decrease in KAT1 current was mainly due to a negative shift in the *I*/V curve along the voltage axis (13), that of AKT1 originated from a decrease in activable channels (Fig. 8*A*). Previous sequence analysis indicated that a putative cyclic nucleotide-binding site sharing sequence homologies with the cyclic nucleotide-binding domain of animal cyclic nucleotide-gated channels is present in both AKT1 and KAT1 polypeptides, downstream of the membrane-spanning region (3, 4). The effect of cGMP on AKT1 and KAT1 activity may thus indicate direct modulation by cGMP, *i.e.* resulting from cGMP binding to the channel. An indirect effect cannot, however, be ruled out since modulation by cyclic nucleotide-dependent protein kinases is a likely means of K^+ channel regulation *in planta* (38). Also, the hypothesis of an indirect effect is supported by the time dependence of the shift in activation potential.

The highest similarities between AKT1 and KAT1 and the animal K^+ channels of the Shaker superfamily are found with the *Drosophila Eag* gene product. The Eag channel has been shown to be both voltage-dependent and cAMP-modulated (39). The existence of a link between strictly voltage-gated K^+ channels and cyclic nucleotide-gated ion channels has been proposed (40). Eag, KAT1, and AKT1 may be members of a class of channels representing such a link.

In conclusion, we have shown that the baculovirus system can be used as an alternative method when expression in *Xenopus* oocytes is unsuccessful for electrophysiological characterization of the ion channel of interest. The plant AKT1 protein has been shown in this way to be a K^+-selective, voltage-gated, and probably cGMP-modulated channel.

Acknowledgment—We thank Dr. David Logan for critical reading of the manuscript.

REFERENCES

1. Lüttge, U., and Clarkson, D. T. (1989) *Prog. Bot.* **50,** 51–73
2. Kochian, L. V., and Lucas, W. J. (1988) *Adv. Bot. Res.* **15,** 93–178
3. Schroeder, J. I., Ward, J. M., and Gassmann, W. (1994) *Annu. Rev. Biophys. Biomol. Struct.* **23,** 441–471
4. Sentenac, H., Bonneaud, N., Minet, M., Lacroute, F., Salmon, J.-M., Gaymard, F., and Grignon, C. (1992) *Science* **256,** 663–665
5. Anderson, J. A., Huprikar, S. S., Kochian, L. V., Lucas, W. J., and Gaber, R. F. (1992) *Proc. Natl. Acad. Sci. U. S. A.* **89,** 3736–3740
6. Müller-Röber, B., Ellenberg, J., Provart, N., Willmitzer, L., Busch, H., Becker, D., Dietrich, P., Hoth, S., and Hedrich, R. (1995) *EMBO J.* **14,** 2409–2416
7. Cao, Y., Ward, J. M., Kelly, W. B., Ichida, A. M., Gaber, R. F., Anderson, J. A., Uozumi, N., Schroeder, J. I., and Crawford, N. (1995) *Plant Physiol.* (*Bethesda*) **109,** 1093–1106
8. Ketchum, K. A., and Slayman, C. W. (1996) *FEBS Lett.* **378,** 19–26
9. Jan, L. Y., and Jan, Y. N. (1992) *Cell* **69,** 715–718
10. Schachtman, D. P., Schroeder, J. I., Lucas, W. L., Anderson, J. A., and Gaber, R. F. (1992) *Science* **258,** 1654–1658
11. Véry, A.-A., Bosseux, C., Gaymard, F., Sentenac, H., and Thibaud, J.-B. (1994) *Pfluegers Arch. Eur. J. Physiol.* **428,** 422–424
12. Véry, A.-A., Gaymard, F., Bosseux, C., Sentenac, H., and Thibaud, J.-B. (1995) *Plant J.* **7,** 321–332
13. Hoshi, T. (1995) *J. Gen. Physiol.* **105,** 309–328
14. Hedrich, R., Moran, O., Conti, F., Bush, H., Becker, D., Gambale, F., Dreyer, I., Küch, A., Neuwinger, K., and Palme, K. (1995) *Eur. Biophys. J.* **24,** 107–115
15. Bertl, A., Anderson, J. A., Slayman, C. L., and Gaber, R. F. (1995) *Proc. Natl. Acad. Sci. U. S. A.* **92,** 2701–2705
16. Nakamura, R. L., McKendree, W. L., Hirsch, R. E., Sedbrook, J. C., Gaber, R. F., and Sussman, M. R. (1995) *Plant Physiol.* (*Bethesda*) **109,** 371–374
17. Basset, M., Conejero, G., Lepetit, M., Fourcroy, P., and Sentenac, H. (1995) *Plant Mol. Biol.* **29,** 947–958
18. Lagarde, D., Basset, M., Lepetit, M., Conejero, G., Gaymard, F., Astruc, S., and

Grignon, C. (1996) *Plant J.* **9,** 195–203
19. Luckow, V. A., and Summers, M. D. (1988) *Bio/Technology* **6,** 47–55
20. Schertler, G. F. X. (1992) *Curr. Opin. Struct. Biol.* **2,** 534–544
21. Klaiber, K., Williams, N., Roberts, T. M., Papazian, D. M., Jan, L. Y., and Miller, C. (1990) *Neuron* **5,** 221–226
22. Li, M., Unwin, N., Stauffer, K. A., Jan, Y. N., and Jan, L. Y. (1994) *Curr. Biol.* **4,** 110–115
23. Santacruz-Toloza, L., Perozo, E., and Papazian, D. M. (1994) *Biochemistry* **33,** 1295–1299
24. Studier, F. W., Rosenberg, A., Dunn, J., and Derbendorff, J. (1990) *Methods Enzymol.* **185,** 60–89
25. Heusterspreute, M., Thi, V. H., Emery, S., Tournis-Gamble, S., Kennedy, N., and Davison, J. (1985) *Gene* (*Amst.*) **39,** 299–304
26. Marston, F. A. O. (1986) *Biochem. J.* **240,** 1–12
27. Davrinche, C., Pasquier, C., Cerutti, M., Serradell, L., Clément, D., Devauchelle, G., Michelson, S., and Davignon, J. L. (1993) *Biochem. Biophys. Res. Commun.* **195,** 469–477
28. Luckow, V. A., and Summers, M. D. (1988) *Virology* **167,** 56–71
29. Schaffner, W., and Weissman, C. (1973) *Anal. Biochem.* **56,** 502–514
30. Laemmli, U. K. (1970) *Nature* **227,** 680–685
31. Garnier, L., Ravallec, M., Blanchard, P., Chaabihi, H., Bossy, J.-P., Devauchelle, G., Jestin, A., and Cerutti, M. (1995) *J. Virol.* **69,** 4060–4068
32. Hamill, O. P., Marty, A., Neher, E., Sakmann, B., and Sigworth, F. J. (1981) *Pfluegers Arch. Eur. J. Physiol.* **391,** 85–100
33. Zittlau, K. E., and Walther, C. (1991) *Pfluegers Arch. Eur. J. Physiol.* **418,** 190–192
34. Stauffer, K. A., Kumar, N. M., Gilula, N. B., and Unwin, N. (1991) *J. Cell Biol.* **115,** 141–150
35. Pajot-Augy, E., Couture, L., Bozon, V., Remy, J.-J., Biache, G., Severini, M., Hurt, J.-C., Pernollet, J.-C., and Salesse R. (1995) *J. Mol. Endocrinol.* **14,** 51–66
36. Brown, A. M. (1993) *Annu. Rev. Biophys. Biomol. Struct.* **22,** 173–198
37. Honoré, E., Attali, B., Romey, G., Lesage, F., Barhanin, J., and Lazdunski, M. (1992) *EMBO J.* **11,** 2465–2471
38. Li, W., Luan, S., Schreiber, S. L., and Assmann, S. M. (1994) *Plant Physiol.* (*Bethesda*) **106,** 957–961
39. Brüggemann, A., Pardo, L. A., Stühmer, W., and Pongs, O. (1993) *Nature* **365,** 445–448
40. Jan, L. Y., and Jan, Y. N. (1990) *Nature* **345,** 672
41. Minet, M., Dufour, M. E., and Lacroute, F. (1992) *Plant J.* **2,** 417–422